Applied Catalysis B: Environmental 182 (2016) 102–108

Contents lists available at ScienceDirect

Applied Catalysis B: Environmental

journal homepage: www.elsevier.com/locate/apcatb

Efficient Ni–Mo hydrodesulfurization catalyst prepared through Keggin polyoxometalate

Ali Alsalme[a], Nabil Alzaqri[a], Ahmad Alsaleh[a], M. Rafiq H. Siddiqui[a,*], Abdullah Alotaibi[b], Elena F. Kozhevnikova[b], Ivan V. Kozhevnikov[b,*]

[a] Department of Chemistry, King Saud University, P.O. Box 2455, Riyadh, Saudi Arabia
[b] Department of Chemistry, University of Liverpool, Liverpool L69 7ZD, United Kingdom

ARTICLE INFO

Article history:
Received 22 July 2015
Received in revised form 28 August 2015
Accepted 2 September 2015
Available online 10 September 2015

Keywords:
Hydrodesulfurization
Thiophene
Polyoxometalates
Ni–Mo catalyst

ABSTRACT

$NiMo/SiO_2$ hydrodesulfurization catalyst prepared through the polyoxometalate route using Keggin type phosphomolybdates has high activity in HDS of thiophene at 350–400 °C and 1 bar pressure. The $NiMo/SiO_2$ pre-catalyst retains intact Keggin structure of phosphomolybdic polyoxometalate, which transforms on stream into a NiMo sulfidic active phase. The pre-catalyst also possesses Brønsted and Lewis acidity, which is lost during the HDS reaction. This catalyst undergoes faster sulfidation and shows higher thiophene conversion and higher butene selectivity than conventional industrial $NiMo/Al_2O_3$ catalyst with similar Mo loading. The polyoxometalate catalyst preparation route is therefore considered to be a performance enhancement methodology for HDS catalysis.

1. Introduction

Hydrodesulfurization (HDS) – the removal of sulfur atoms from sulfur-containing molecules in petroleum feedstocks by hydrotreatment – is one of the most important processes of the petroleum refining industry, which is employed to upgrade the quality of fuels [1,2]. It is driven by ever stringent environmental legislation demanding very low sulfur levels in fuels. Current HDS technology employs sulfided Co(Ni)Mo/Al_2O_3 catalysts [1–3]. Research into improvement of activity and selectivity of HDS catalysts continues globally at a fast pace. This, among others, includes the development of new methods of preparation of Co(Ni)Mo catalysts, for example, Co chemical vapor deposition [4], addition of citric acid [5] and phosphorus [4], the use of new active phases for HDS catalysts, such as noble metals [6], transition metal carbides [7], nitrides [8] and phosphides [9,10].

The Co(Ni)Mo/Al_2O_3 catalysts are obtained by sulfidation of an oxide precursor (pre-catalyst), which is usually prepared by impregnation of γ-alumina support with an aqueous solution containing ammonium heptamolybdate and Co(II) or Ni(II) nitrate as a promoter, often with addition of phosphoric acid as a modifier [1–3]. When both molybdate and phosphate are present, the impregnation solution contains P–Mo heteropoly anions such as $P_2Mo_5O_{23}^{6-}$, $PMo_9O_{31}(OH)_3^{6-}$, $PMo_{11}O_{39}^{7-}$, $PMo_{12}O_{40}^{3-}$, and $P_2Mo_{18}O_{62}^{6-}$, depending on the pH and P and Mo concentrations [2]. This has stimulated direct use of heteropoly compounds for the preparation of oxide precursors for HDS catalysts [11–21]. Heteropoly compounds, also known as polyoxometalates [22], have found many applications in catalysis, including several large-scale industrial processes [23–25]. Most frequently, readily available water-soluble Keggin type heteropoly compounds comprising heteropoly anions of the composition $XM_{12}O_{40}^{n-}$ ($M = Mo^{6+}$, W^{6+}; $X = P^{5+}$, Si^{4+}) have been used for the preparation of HDS pre-catalysts, with Co(II) and/or Ni(II) included as the counter cations or addenda atoms. This preparation methodology has several advantages [16,17]: (1) incorporation of all the elements required for HDS catalyst within heteropoly compound allowing the preparation of oxide precursor in a single impregnation step; (2) intimate interaction between the key elements in oxide precursor and finished sulfided catalyst; and (3) extraneous counter ions such as NH_4^+ can be excluded from the impregnation solution. It has been found that CoMo catalysts prepared through the polyoxometalate route show higher activity in HDS of thiophene than the conventional CoMo catalysts, which has been attributed to better interaction between the oxomolybdenum phase and the Co promoter [16]. In HDS of dibenzothiophene, non-promoted phosphotungstic heteropoly acid $H_3PW_{12}O_{40}$ has been found to exhibit a close activity

* Corresponding authors at: Department of Chemistry, University of Liverpool, Liverpool L69 7ZD, United Kingdom.
E-mail addresses: rafiqs@ksu.edu.sa (M.R.H. Siddiqui), kozhev@liverpool.ac.uk (I.V. Kozhevnikov).

http://dx.doi.org/10.1016/j.apcatb.2015.09.018
0926-3373/

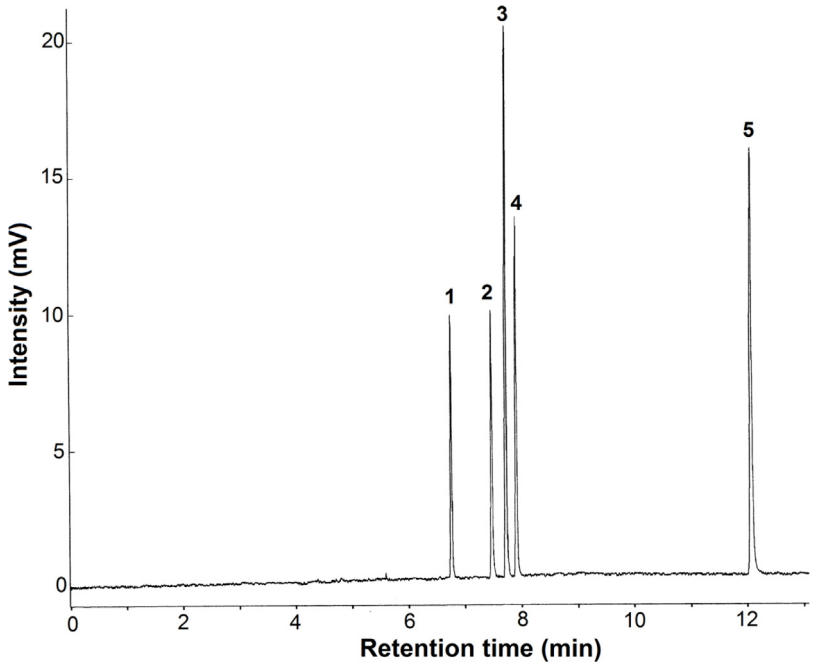

Fig. 1. GC trace for thiophene HDS over Ni_3–PMo (400 °C, 0.20 g catalyst amount, 2.63 kPa thiophene partial pressure in H_2 flow, 20 mL min^{-1} flow rate, space time W/F = 152 g h mol^{-1}, ambient pressure; 76% thiophene conversion): (1) *n*-butane, (2) 1-butene, (3) *trans*-2-butene, (4) *cis*-2-butene, (5) thiophene; 60 m × 0.32 mm GS-GasPro capillary column; flame ionization detector.

to the conventional industrial CoMo catalyst without evidence of deactivation [15].

In this work, we explore the activity of silica-supported nickel phosphomolybdate catalysts prepared from Ni(II) salts of phosphomolybdic acid $H_3PMo_{12}O_{40}$ (HPMo) in the HDS of thiophene. This reaction is relevant to the hydrotreating of FCC naphtha aiming at thiophene removal with a minimal hydrogenation of alkenes present in the naphtha to avoid loss of octane rating of the final gasoline pool [2]. Catalyst selectivity is the key to this task; it requires the catalysts with high HDS and low alkene hydrogenation activity. Our aim is to investigate the effect of Ni(II) substitution in HPMo on the catalytic activity and selectivity, the role of Brønsted and Lewis acidity of the pre-catalyst in the HDS process and to get an insight into Ni(II)–HPMo pre-catalyst evolution in the course of thiophene HDS.

2. Experimental

2.1. Chemicals and materials

Phosphomolybdic acid hydrate $H_3Mo_{12}PO_{40}{\cdot}20H_2O$, $Ni(NO_3)_2{\cdot}6H_2O$ and thiophene (99%) were from Sigma–Aldrich and Aerosil 300 silica support (S_{BET} = 300 m^2 g^{-1}) from Degussa.

2.2. Preparation of HDS pre-catalysts

Silica-supported $H_3PMo_{12}O_{40}$ pre-catalyst, HPMo/SiO_2, with 15 wt% HPMo loading based on anhydrous HPMo was prepared by wet impregnation of SiO_2 with $H_3PMo_{12}O_{40}$ in aqueous slurry at 40–50 °C with continuous stirring for 24 h. Solid residue was isolated through rotary evaporation at 45 °C, dried under vacuum at 150 °C and calcined at 300 °C under nitrogen flow for 3 h with a heating rate of 5 °C min^{-1}. The pre-catalyst was then ground into a powder with a particle size of 45–180 μm.

Silica-supported Ni(II) phosphomolybdate pre-catalysts with Ni(II)/HPMo molar ratios of 1:1, 2:1 and 3:1 (i.e., Ni/Mo atomic ratios of 1:12, 1:6 and 1:4) and a Ni(II)–HPMo loading of 15 wt% (13% MoO_3) were prepared similarly by wet impregnation of SiO_2 with HPMo and the required amounts of $Ni(NO_3)_2$ from aqueous solution, followed by isolation, drying and calcination at 300 °C as above. The Ni(II)–HPMo loading was confirmed by ICP analysis. Hereafter, these pre-catalysts are designated as Ni–PMo, Ni_2–PMo and Ni_3–PMo, respectively.

Industrial $NiMo/Al_2O_3$ pre-catalyst (ICI Catalyst 61-1, Ni/Mo = 0.62 mol/mol), containing NiO (3.8%), MoO_3 (11.8%), SiO_2 (1.8%) and γ-Al_2O_3 (balance) [3], was crushed and sieved into a powder with a particle size of 45–180 μm. It had a surface area of 220 m^2 g^{-1} and a pore volume of 0.6 cm^3 g^{-1} [3].

2.3. Techniques

Catalyst surface area, pore volume and pore size were determined on a Micromeretics ASAP 2010 instrument by measuring nitrogen adsorption at −196 °C. Before measurement the catalysts were pre-treated at 250 °C in vacuum. Powder X-ray diffractograms were collected on a PANalytical Xpert diffractometer using CuKα radiation (λ = 0.1542 nm). ICP-AES analysis of sulphur was carried out on a Spectro Ciros emission spectrometer. Fourier transform infrared spectra (FTIR) of pre-catalysts and spent catalysts were recorded on a Nicolet Nexus FTIR spectrometer using powdered catalyst mixtures with KBr. Silica absorption was subtracted using a silica–KBr mixture as the background. DRIFTS (diffuse reflectance infrared Fourier transform spectra) of adsorbed pyridine were taken on the same spectrometer. Catalyst samples were ground with KBr (1–10 wt% in KBr) and pre-treated at 150 °C/10^{-3} kPa for 1 h. The samples were then exposed to pyridine vapor at room temperature for 1 h, followed by pumping out at 150 °C/10^{-3} kPa for 1 h to remove physisorbed pyridine. Then the DRIFT spectra of adsorbed pyridine were recorded at room temperature at a resolution of 4 cm^{-1}. Temperature programmed reduction (H_2–TPR) of catalysts was carried out on a Micromeritics TPD/TPR 2900 apparatus equipped with a thermal conductivity detector. Catalyst samples (20–30 mg) were heated up to 900 °C at a rate of 10 °C min^{-1} in a H_2–N_2 (5:95) gas flow (60 mL min^{-1}).

Table 1
Texture of Ni phosphomolybdate pre-catalysts.

Catalyst[a]	S_{BET}[b] ($m^2\ g^{-1}$)	Pore volume[c] ($cm^3\ g^{-1}$)	Pore diameter[d] (Å)
HPMo	200	0.47	94
Ni–PMo	197	0.48	96
Ni_2–PMo	182	0.45	98
Ni_3–PMo	192	0.48	100

[a] Silica-supported pre-catalysts with 15 wt% HPMo or Ni(II)–HPMo loading on Aerosil 300 (S_{BET} = 300 $m^2\ g^{-1}$).
[b] BET surface area.
[c] Single point total pore volume at relative pressure P/P_o = 0.97.
[d] Average pore diameter.

2.4. Catalyst testing

The gas-phase hydrodesulfrization of thiophene was carried out in flowing H_2 at 350–400 °C under atmospheric pressure in a down-flow quartz fixed-bed reactor (9 mm i.d.) with online GC analysis (Varian 3800 instrument with a 30 m × 0.25 mm × 0.5 μm HP-INNOWAX capillary column and a flame ionization detector). For more accurate analysis of C_1–C_4 hydrocarbon products, a 60 m × 0.32 mm GS-GasPro capillary column was used, which allowed for complete separation of these hydrocarbons (Fig. 1). The temperature in the reactor was controlled by a Eurotherm controller using a thermocouple placed at the top of the catalyst bed. Thiophene was fed by passing hydrogen flow controlled by a Brooks mass flow controller through a stainless steel saturator which held liquid thiophene at 0 °C to keep the chosen thiophene partial pressure of 2.63 kPa in hydrogen flow [26]. The reactor was packed with 0.20 g of pre-catalyst powder of 45–180 μm particle size. The gas feed entered the reactor at the top at a flow rate of 20 mL min^{-1} (space time W/F = 152 g h/mol, where W (g) is the catalyst weight and F (mol h^{-1}) is the molar flow rate of thiophene), unless stated otherwise. Prior to reaction monitoring, the pre-catalysts were pre-treated (pre-sulfided) in situ in the feed flow containing thiophene (2.63 kPa) in H_2 for 1–3 h at the reaction temperature (3 h at 350–370 °C and 1 h at 400 °C). Once reaction started, the downstream flow was analyzed by the on-line GC to continuously monitor thiophene conversion. Product selectivity was determined at selected times on stream by GC using the GS-GasPro capillary column. The selectivity was defined as the percentage of thiophene converted into a particular product and quoted in molar per cent. The mean absolute percentage error in conversion and selectivity was ≤5% and the carbon balance was maintained within 95%.

3. Results and discussion

3.1. Pre-catalyst characterization

Silica-supported Ni(II)–HPMo catalyst precursors prepared through Keggin P–Mo polyoxometalates incorporated all the elements required for HDS process within polyoxometalate structure, i.e., the catalyst (Mo), the promoter (Ni) and the modifier (P). Although in industry γ-alumina is the preferred support for HDS catalysts for its high mechanical strength and stability, in our study we chose silica as an inert support. This is because alumina is well known for its strong interaction with polyoxometalates [23–25] and it also possesses considerable Brønsted and Lewis acidity, which would make monitoring catalyst evolution during the HDS process more difficult. The Ni(II)–HPMo/SiO_2 pre-catalysts were mesoporous materials with a BET surface area of 182–200 $m^2\ g^{-1}$, 0.45–0.48 $cm^3\ g^{-1}$ pore volume and 94–100 Å pore diameter (Table 1). The pre-catalyst with a sub-stoichiometric Ni(II)/HPMo molar ratio of 1:1 may be viewed as the partially substituted heteropoly salt $Ni^{II}H[PMo_{12}O_{40}]$. For over-stoichiometric Ni(II)/HPMo ratios 2:1 and 3:1, the pre-catalysts probably comprise a mixture of a Ni(II) salt of HPMo and NiO on the silica surface, as excess Ni(II) nitrate would decompose to form NiO upon calcination at 300 °C: $Ni(NO_3)_2 \rightarrow NiO + 2NO_2 + O_2$ [27].

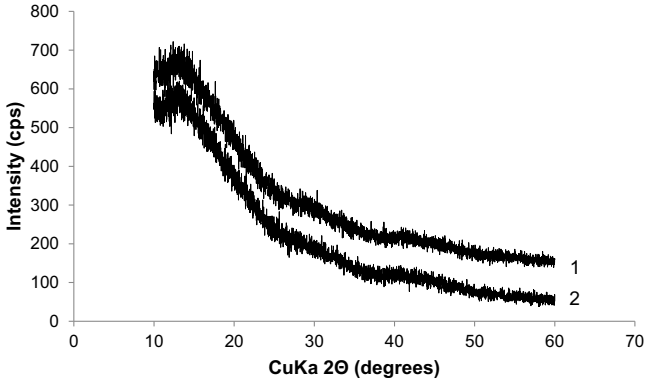

Fig. 2. XRD for Ni_3–PMo pre-catalyst (1) and spent catalyst (2).

All the pre-catalysts were found to be amorphous materials, as exemplified in Fig. 2 showing the XRD for Ni_3–PMo. This is not unexpected since heteropoly compound crystal phase in silica-supported catalysts usually shows above 20 wt% loading [23–25].

The Keggin primary structure of P–Mo heteropoly anions remained intact in these materials, as demonstrated by FTIR. Fig. 3 shows the DRIFT spectrum of Ni_3–PMo (powdered with KBr), with the strong absorption band of silica at 1100 cm^{-1} largely subtracted. It matches quite well the infrared spectra of bulk $H_3PMo_{12}O_{40}$ and its salts (cm^{-1}): 1062–1068 (P—O), 954–963 (Mo═O), 869–880 (Mo—O—Mo corner-sharing) and 785–805 (Mo—O—Mo edge-sharing) [28]. In the Ni_3–PMo spectrum, the P—O band showing a peak at 1048 cm^{-1} is partly obscured by the SiO_2 band at 1100 cm^{-1}.

The composition of the Ni(II)–HPMo pre-catalysts implies that they should possess Brønsted and Lewis acidity owing to the presence of heteropoly acid protons and Ni(II). Indeed, all these materials show the characteristic peaks of Brønsted (~1540 cm^{-1}) and Lewis (~1450 cm^{-1}) acid sites in their DRIFT spectra of adsorbed pyridine, together with the band at 1490 cm^{-1} attributed to both types of acid sites [29] (Fig. 4). As expected, the ratio of Brønsted and Lewis site densities (B/L) decreases with increasing the Ni(II)/HPMo ratio (Table 2). The B/L values were calculated from integral intensities of the corresponding bands, assuming equal extinction coefficients for these bands [29]. Both Brønsted and Lewis acidity was lost during the HDS reaction as a result of catalyst sulfidation (see below).

Fig. 5 shows temperature programmed reduction (H_2–TPR) of the Ni(II)–HPMo pre-catalysts. All of them, including the non-promoted HPMo, exhibit two reduction peaks at 639–646 and 778–810 °C. The Keggin structure of HPMo would probably collapse to form MoO_3 and P_2O_5 before the reduction took place. These peaks can be attributed to reduction of Mo(VI) to Mo(IV). As Mo(VI)

Table 2
Brønsted (B) and Lewis (L) acidity of Ni phosphomolybdate pre-catalysts from DRIFT spectroscopy of adsorbed pyridine.

Catalyst	Acid site type	B/L
HPMo	B + L	1.36
Ni–PMo	B + L	0.34
Ni_2–PMo	B + L	0.39
Ni_3–PMo	B + L	0.20
Ni_3–PMo[a]	None	–

[a] Spent catalyst.

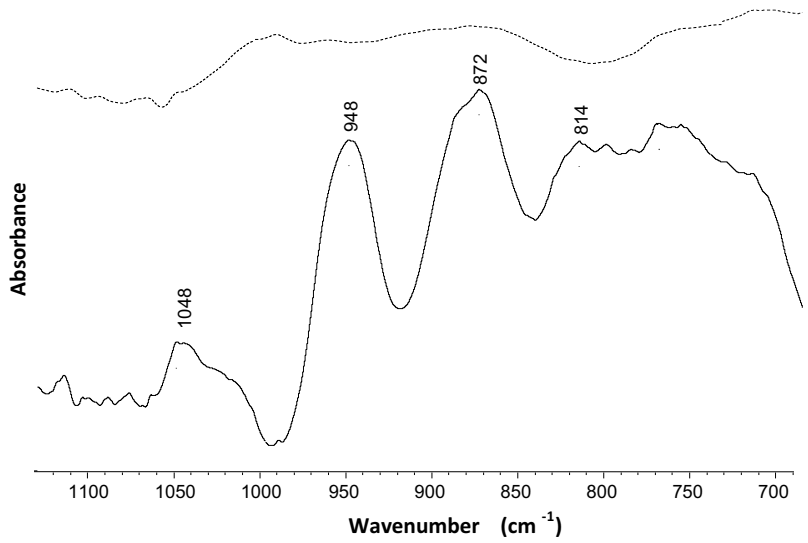

Fig. 3. FTIR spectra of Ni_3–PMo pre-catalyst (solid line) and spent catalyst (dashed line).

is in large excess over Ni(II) in the Ni(II)–HPMo pre-catalysts, reduction of Ni(II) is probably masked by the Mo peaks. Very similar H_2–TPR profiles have been reported previously for non-promoted HPMo/TiO_2 [17], MoO_3/SiO_2 and NiO–MoO_3/SiO_2–Al_2O_3 [30].

3.2. Catalyst performance in HDS of thiophene

Catalyst testing included pre-sulfidation with reaction feed at reaction temperature for 1–3 h. After that thiophene conversion and reaction selectivity were monitored as a function of time on stream. At 350 °C, it took about 3 h to complete catalyst pre-sulfidation and reach steady state, whereas at 400 °C, the pre-sulfidation was complete in 1 h to achieve steady thiophene conversion. Selected spent catalysts were characterized by XRD and FTIR to monitor their structure and acidity and by elemental analysis for sulfur content and coking (Section 3.3). Initial testing at 350 °C and 2 h time on stream showed that the HDS activity of the nickel phosphomolybdate catalysts prepared through the polyoxometalate route predictably increased with increasing the Ni/Mo molar ratio. Representative results are given in Table 3 and Fig. 6. The most active catalyst Ni_3–PMo was tested further at different temperatures and longer time on stream and also characterized after reaction.

With Ni_3–PMo, thiophene conversion increased from 50 to 75% with increasing the temperature from 350 to 400 °C (Table 3). At 400 °C and space time $W/F = 152$ g h mol^{-1}, the catalyst showed stable performance with average thiophene conversion of 75% for 8 h

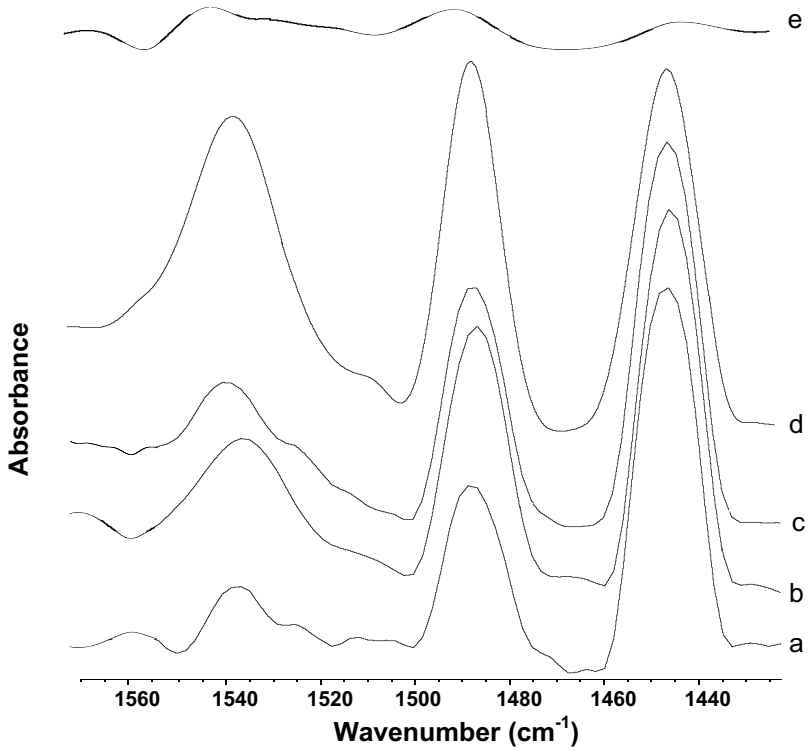

Fig. 4. DRIFT spectra of adsorbed pyridine: (a) Ni_3–PMo, (b) Ni_2–PMo and (c) Ni–PMo, (d) HPMo, (e) spent Ni_3–PMo catalyst.

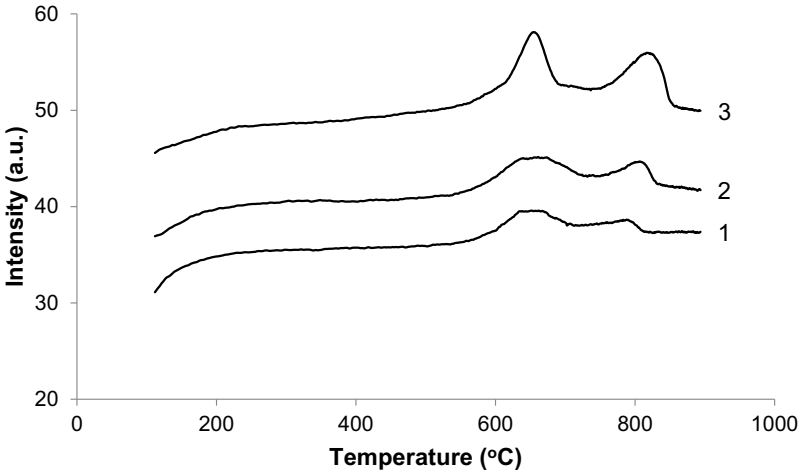

Fig. 5. H_2–TPR for pre-catalysts: (1) Ni_2–PMo, (2) Ni–PMo and (3) HPMo.

Table 3
HDS of thiophene over Ni phosphomolybdate catalysts.[a]

Catalyst	Temperature(°C)	Conversion[b](%)	Selectivity (%)			
			Butane	1-butene	*trans*-2-butene	*cis*-2-butene
HPMo	350	2 (2)				
Ni–PMo	350	3 (2)				
Ni_2–PMo	350	33 (2)	12	24	35	29
Ni_3–PMo	350	50 (2)	14	25	34	27
Ni_3–PMo	370	69 (2)	15	23	37	25
Ni_3–PMo[c]	400	75 (8)	18	19	38	25
Ni_3–PMo[d]	400	90 (8)	28	13	22	16
NiMo (ICI 61-1)[e]	400	42 (8)	24	15	37	24

[a] 0.20 g catalyst amount, 2.63 kPa thiophene partial pressure in H_2 flow, 20 mL min^{-1} flow rate, space time W/F = 152 g h mol^{-1}, ambient pressure, catalyst pre-sulfidation at reaction temperature (3 h at 350–370 °C and 1 h at 400 °C).
[b] Average conversion of thiophene during time on stream (h) given in round brackets.
[c] 0.58% coke and 7.0% sulfur content in the catalyst after reaction.
[d] W/F = 304 g h mol^{-1}.
[e] 0.19% coke and 3.8% sulfur content in the catalyst after reaction.

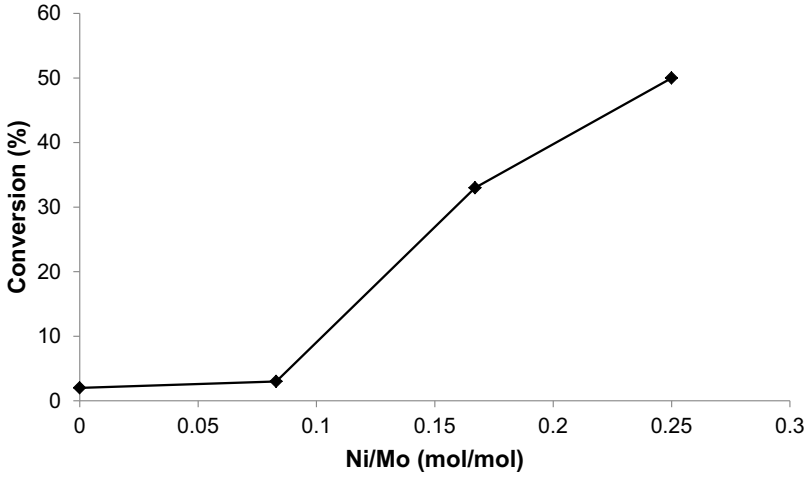

Fig. 6. Thiophene conversion versus Ni/Mo molar ratio for HDS of thiophene (2.63 kPa partial pressure) over Ni(II)–HPMo catalysts (0.20 g) at 350 °C, 20 mL min^{-1} H_2 flow rate, space time W/F = 152 g h mol^{-1}, ambient pressure, 3 h pre-sulfidation time at 350 °C, 2 h time on stream.

on stream without deactivation (Fig. 7). Increasing the space time to 304 g h mol^{-1} led to an increase in thiophene conversion to 90% without catalyst deactivation for at least 8 h on stream (Table 3). *n*-Butene isomers (1-butene, *trans*-2-butene and *cis*-2-butene), were the main reaction products at a total selectivity of 72–82% at 400 °C with *n*-butane also formed via butene hydrogenation (Eq. (1)).

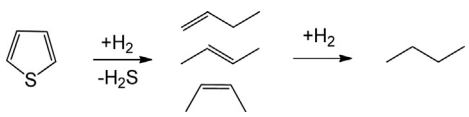

(1)

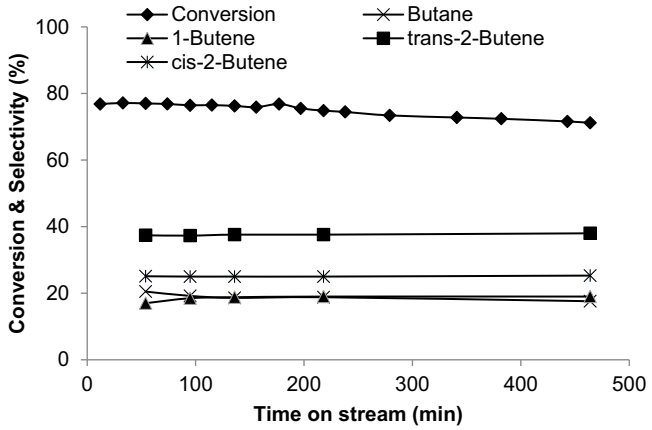

Fig. 7. Time course for HDS of thiophene (2.63 kPa partial pressure) over Ni_3–PMo (0.20 g) at 400 °C, 20 mL min^{-1} H_2 flow rate, space time W/F = 152 g h mol^{-1}, ambient pressure, 1 h pre-sulfidation time at 400 °C.

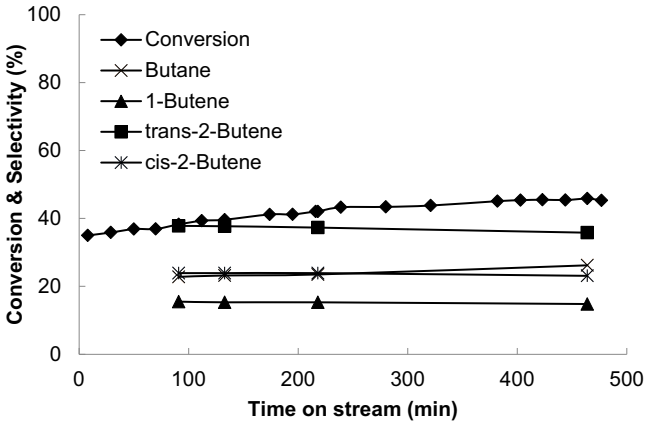

Fig. 8. Time course for HDS of thiophene (2.63 kPa partial pressure) over industrial NiMo/γ-Al_2O_3 catalyst ICI 61-1 (0.20 g) at 400 °C, 20 mL min^{-1} H_2 flow rate, space time W/F = 152 g h mol^{-1}, ambient pressure, 1 h pre-sulfidation time at 400 °C.

Despite considerable acidity of the Ni_3–PMo pre-catalyst (Table 2), neither isobutene nor isobutane was observed among the products, which indicates the lack of skeletal isomerization in the system. In addition, no C_1–C_3 cracking by-products was observed, as demonstrated by the GC trace (Fig. 1), where these by-products would appear at retention times from 4 to 6 min. These results can be explained by the loss of catalyst acidity upon sulfidation (see below).

It appears that redox behavior of the Ni(II)–HPMo pre-catalysts in H_2–TPR (Fig. 5) does not correlate with their performance in the HDS of thiophene. The HDS reaction proceeds at temperatures (350–400 °C) that are much lower than those of the H_2–TPR (600–800 °C), which implies that sulfidation of these pre-catalysts to form catalytically active phases occurs at lower temperatures as compared to the H_2–TPD. It should be noted, however, that the H_2–TPR was carried out under transient conditions. Slow isothermal catalyst reduction with H_2 may be possible at lower temperatures below 600 °C.

Further mechanistic evidence was obtained from thermodynamic analysis of reaction products. The equilibrium ratio of *n*-butene isomers has been found to be 1-butene/*trans*-2-butene/*cis*-2-butene = 1:1.8:1.2 at 400 °C and 1 bar [31]. This is very close to the ratio obtained here with Ni_3–PMo (Table 3), which shows that the butenes produced were at equilibrium. On the other hand, hydrogenation of butenes to *n*-butane was far from equilibrium. The Gibbs free energy for the hydrogenation of 1-butene, *trans*-2-butene and *cis*-2-butene was calculated from the data [32,33] to be −36.7, −31.8 and −34.2 kJ mol^{-1}, respectively, at 400 °C and 1 bar for ideal gas mixture. The corresponding values of equilibrium constant K_p are 710, 290 and 450 bar^{-1}. At $[H_2] \gg [C_4H_8]$ and $[H_2] \gg [C_4H_{10}]$, as in our reaction system, these values are practically equal to the equilibrium molar ratios of *n*-butane to the corresponding butenes, i.e., *n*-butane/1-butene, *n*-butane/*trans*-2-butene and *n*-butane/*cis*-2-butene, respectively. In fact, the experimental ratios are 2–3 orders of magnitude lower (Table 3). This indicates that butene-to-butane hydrogenation is a slow process, i.e., Ni_3–PMo catalyst, to its advantage, has a relatively low alkene hydrogenation activity. As a result, *n*-butane selectivity predictably increases with thiophene conversion.

Although the HDS mechanism of thiophene at low pressure is under debate [2], it may tentatively be represented by Scheme 1 via hydrogenation of thiophene to tetrahydrothiophene followed by H_2S elimination to give butadiene, which is hydrogenated to butenes and further to *n*-butane [2]. Our results indicate that with Ni_3–PMo catalyst the formation of butenes is a fast and probably reversible step, whereas subsequent hydrogenation to *n*-butane is a slow step. As in many previous reports, neither tetrahydrothiophene nor butadiene was found in our reaction system probably because they react quickly once formed [2].

For comparison, an industrial oxide pre-catalyst NiMo/γ-Al_2O_3 (ICI Catalyst 61-1) with similar Mo loading but a higher Ni/Mo molar ratio of 0.62 [3] was tested under the same conditions at W/F = 152 g h mol^{-1}. This catalyst, despite its higher Ni loading and Ni/Mo ratio, showed a lower thiophene conversion of 42% compared to the Ni_3–PMo (75%) per equal catalyst weight (Table 3). In spite of the lower thiophene conversion, the ICI catalyst also gave a lower butene selectivity (76% versus 82%), thus exhibiting higher alkene hydrogenation activity compared to Ni_3–PMo. This can be explained by the higher Ni content in the ICI catalyst. Fig. 8 shows the HDS time course for this catalyst. Interestingly, it takes 6 h for the ICI catalyst to reach steady state after 1 h pre-sulfidation at 400 °C, which implies that its sulfidation occurs slower in comparison with the Ni_3–PMo catalyst (Fig. 7). This may be explained by the well-known lability of Keggin phosphomolybdates [25].

Overall, these results demonstrate that the Ni_3–PMo catalyst prepared through the polyoxometalate route has enhanced HDS performance compared to the conventional industrial catalyst. The Ni_3–PMo catalyst has the potential of reducing hydrogen consumption in HDS process and the loss of high octane alkenes in the final gasoline pool. The higher activity of Ni_3–PMo can be attributed to close interaction between oxomolybdenum species and Ni promoter and to the presence of phosphorus modifier in this catalyst.

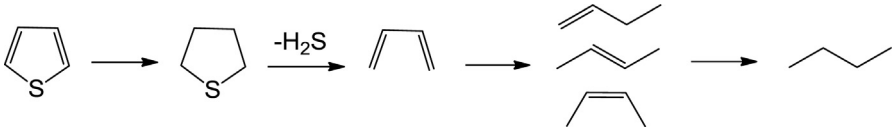

Scheme 1. Mechanism of HDS of thiophene.

3.3. Characterization of sulfided Ni_3–PMo catalyst

This section describes post-reaction characterization of the Ni_3–PMo catalyst, which showed the highest HDS activity (Table 3). All Ni(II)–HPMo pre-catalysts, initially lightly colored, turned pitch-black after reaction, which indicates their sulfidation. After 8 h on stream at 400 °C, the Ni_3–PMo catalyst contained only a small amount of coke (0.58 wt% carbon content). The sulfur content was found to be 7.0 wt%, which was largely accumulated during 1 h pre-sulfidation. This corresponds to 97% catalyst sulfidation as estimated assuming the formation of MoS_2 and NiS and implies almost complete transformation of the Ni(II)–HPMo pre-catalyst into an active metal sulfide phase on the silica surface.

From XRD, the spent Ni_3–PMo catalyst was an amorphous material like the Ni_3–PMo pre-catalyst (Fig. 2). As the result of sulfidation, the Keggin structure of P–Mo polyoxometalate was completely destroyed. This is clearly indicated by FTIR spectroscopy, which shows that the infrared bands characteristic of Keggin structure, that are seen in the spectrum of Ni_3–PMo pre-catalyst, disappeared after catalyst sulfidation (Fig. 3).

The role of Brønsted and Lewis acid sites in HDS catalysts prepared through the polyoxometalate route is one of the objectives of this study. As stated in Section 3.1, polyoxometalate pre-catalysts possess significant Brønsted and Lewis acidity, which might affect the selectivity of HDS process by enhancing cracking and isomerization of hydrocarbon products. However, the DRIFT spectroscopy of adsorbed pyridine showed that sulfided Ni_3–PMo catalyst exhibited neither Brønsted nor Lewis acidity strong enough to interact with pyridine, (Fig. 4). The loss of acidity explains the lack of cracking and skeletal isomerization activity of this catalyst in thiophene HDS. Therefore, one can conclude that the acidity of the polyoxometalate pre-catalysts is largely irrelevant to the HDS process; it will be gone after catalyst sulfidation and not affect the HDS process after reaction steady state has been reached.

Therefore, from the post-reaction catalyst characterization, the initial Ni(II)–HPMo polyoxometalate pre-catalyst transforms into an active metal sulfide phase in the course of thiophene HDS. Previously, non-promoted $H_3PW_{12}O_{40}$ has been found to decompose upon the HDS of dibenzothiophene as evidenced by ^{31}P MAS NMR [15]. Sulfidation of the Ni(II)–HPMo pre-catalyst was found to occur easier compared to the industrial $NiMo/Al_2O_3$ oxide catalyst (cf. Figs. 6 and 8). The opposite has been found for the more stable $H_3PW_{12}O_{40}$ as compared to the industrial $CoMo/Al_2O_3$ oxide catalyst [15].

4. Conclusions

It has been demonstrated that the $NiMo/SiO_2$ HDS catalyst (Ni/Mo = 0.25 mol/mol) prepared through the polyoxometalate route using Keggin type phosphomolybdates has high activity in the HDS of thiophene. Compared to the industrial $NiMo/Al_2O_3$ catalyst with similar Mo loading and a higher Ni/Mo ratio of 0.62, the new catalyst undergoes faster sulfidation and shows higher thiophene conversion and higher butene selectivity. This catalyst has the potential of reducing hydrogen consumption in HDS process and the loss of high octane alkenes in the final gasoline pool. On the basis of these results, the polyoxometalate catalyst preparation route is considered to be a performance enhancement methodology for HDS catalysis.

Acknowledgements

This research was funded by the National Plan for Science, Technology and Innovation (MAARIFAH), King Abdulaziz City for Science and Technology, Saudi Arabia, Award No. 11-NAN-1852-02. We thank Shaqra University, Shaqra, Saudi Arabia for PhD. studentship (A. Alotaibi).

References

[1] I.V. Babich, J.A. Moulijn, Fuel 82 (2003) 607–631.
[2] R. Prins, in: G. Ertl, H. Knözinger, F. Schüth, J. Weitkamp (Eds.), Handbook of Heterogeneous Catalysis, 6, Wiley-VCH, 2008, pp. 2695–2718.
[3] P.J.H. Carnell, in: M.V. Twigg (Ed.), Catalyst Handbook, Wolfe Publishing, London, 1989, pp. 204–208.
[4] Y. Okamoto, Catal. Today 132 (2008) 9–17.
[5] N. Rinaldi, K. Usman, T. Al-Dalama, Y. Kubota, Okamoto, Appl. Catal. A 360 (2009) 130–136.
[6] A. Niquille-Röthlisberger, R. Prins, Catal. Today 123 (2007) 198–207.
[7] M. Lewandowski, A. Szymaínska-Kolasa, P. Da Costa, C. Sayag, Catal. Today 119 (2007) 31–34.
[8] M. Nagai, Appl. Catal. A 322 (2007) 178–190.
[9] Y. Kanda, C. Temma, A. Sawada, M. Sugioka, Y. Uemichi, Appl. Catal. A 475 (2014) 410–419.
[10] R. Prins, M.E. Bussell, Catal. Lett. 142 (2012) 1413–1436.
[11] S. Damyanova, A. Spojakina, D. Shopov, Appl. Catal. 48 (1989) 177–186.
[12] A.M. Maitra, N.W. Cant, D.L. Trimm, Appl. Catal. 48 (1989) 187–197.
[13] A. Griboval, P. Blanchard, L. Gengembre, E. Payen, M. Fournier, J.L. Dubois, J.R. Bernard, J. Catal. 188 (1999) 102–110.
[14] C.I. Cabello, I.L. Botto, H.J. Thomas, Appl. Catal. A 197 (2000) 79–86.
[15] R. Shafi, M.R.H. Siddiqui, G.J. Hutchings, E.G. Derouane, I.V. Kozhenikov, Appl. Catal. A 204 (2000) 251–256.
[16] A. Griboval, P. Blanchard, E. Payen, M. Fournier, J.L. Dubois, J.R. Bernard, Appl. Catal. A 217 (2001) 173–183.
[17] E. Kraleva, A. Spojakina, K. Jiratova, L. Petrov, Catal. Lett. 112 (2006) 203–212.
[18] R. Palcheva, A. Spojakina, K. Jiratova, L. Kaluza, Catal. Lett. 137 (2010) 216–223.
[19] K. Ben Tayeb, C. Lamonier, C. Lancelot, M. Fournier, A. Bonduelle-Skrzypczak, F. Bertoncini, Appl. Catal. B 126 (2012) 55–63.
[20] P.A. Nikul'shin, A.V. Mozhaev, D.I. Ishutenko, P.P. Minaev, A.I. Lyashenko, A.A. Pimerzin, Kinet. Catal. 53 (2012) 620–631.
[21] F.J. Méndez, A. Llanos, M. Echeverría, R. Jáuregui, Y. Villasana, Y. Díaz, G. Liendo-Polanco, M.A. Ramos-García, T. Zoltan, J.L. Brito, Fuel 110 (2013) 249–258.
[22] M.T. Pope, Heteropoly and Isopoly Oxometalates, Springer, Berlin, 1983.
[23] T. Okuhara, N. Mizuno, M. Misono, Adv. Catal. 41 (1996) 113–252.
[24] I.V. Kozhevnikov, Chem. Rev. 98 (1998) 171–198.
[25] I.V. Kozhevnikov, Catalysis by Polyoxometalates, Wiley & Sons, Chichester, 2002.
[26] D.R. Stull, Ind. Eng. Chem. 39 (1947) 517–550.
[27] S. Yuvaraj, L. Fan-Yuan, C. Tsong-Huei, Y. Chuin-Tih, J. Phys. Chem. B 107 (2003) 1044–1047.
[28] C. Rocchiccioli-Deltcheff, M. Fournier, R. Franck, R. Thouvenot, Inorg. Chem. 22 (1983) 207–216.
[29] H. Knözinger, in: G. Ertl, H. Knözinger, F. Schüth, J. Weitkamp (Eds.), Handbook of Heterogeneous Catalysis, 2, Wiley-VCH, 2008, p. 1154.
[30] J. Brito, J. Laine, Polyhedron 5 (1986) 179–182.
[31] J. Happel, M.A. Hnatow, R. Mezaki, J. Chem. Eng. Data 16 (1971) 206–209.
[32] S.S. Chen, R.C. Wilhoit, B.J. Zwolinski, J. Phys. Chem. Ref. Data 4 (1975) 859–869.
[33] R.A. Alberty, C.A. Gehrig, J. Phys. Chem. Ref. Data 14 (1985) 803–820.